The Local Structures of Silver(I) Ion Catalysts Anchored within Zeolite Cavities and Their Photocatalytic Reactivities for the Elimination of N_2O into N_2 and O_2

Woo-Sung Ju, Masaya Matsuoka, Kiyoshi Iino, Hiromi Yamashita, and Masakazu Anpo*

Department of Applied Chemistry, Graduate School of Engineering, Osaka Prefecture University, 1-1 Gakuen-cho, Sakai, Osaka 599-8531, Japan

Received: February 28, 2003

Ag^+/ZSM-5 catalysts were prepared by an ion-exchange method and characterized by in-situ XPS, XAFS (XANES and EXAFS), UV−Vis, photoluminescence, and FT-IR investigations. These Ag^+/ZSM-5 catalysts were found to exhibit an UV absorption band at around 190 nm due to the isolated Ag^+ ions. The addition of N_2O molecules leads to a shift in this band to 220 nm due to the adsorption of N_2O on the Ag^+ ions. The adsorption of N_2O on the Ag^+ ions could also be clarified by the appearance of characteristic FT-IR bands at 2251 cm^{-1}. UV irradiation of the Ag^+/ZSM-5 catalysts in the presence of N_2O led to the photocatalytic decomposition of N_2O into N_2 and O_2 at temperatures as low as 298 K. It was found that UV light at around 200−250 nm is effective for the reaction, suggesting that excitation of the isolated Ag^+ ion plays a significant role in the photocatalytic decomposition of N_2O.

Introduction

The removal of nitrous oxide (N_2O) from the exhaust of internal combustion engines or industrial boilers is one of the most urgent issues needing to be solved since the serious effects of N_2O not only are a health problem but also lead to the destruction of the ozonosphere and are a leading factor in the greenhouse effect.[1−3] Many studies have focused on the search for efficient catalysts aimed at effective N_2O decomposition, and it has been reported that zeolite catalysts which have been ion-exchanged or supported with Rh or Fe ions are effective for the direct decomposition and also the selective catalytic reduction (SCR) of N_2O at low temperatures of around 523 K.[4−7]

On the other hand, the application of photocatalysts for N_2O elimination is also significant and desirable in terms of the utilization of abundant solar energy and easy operation even under ambient temperatures. It is known that semiconducting titanium oxides (TiO_2) can decompose N_2O photocatalytically, where the electron and hole produced by light adsorption play a significant role.[8,9] However, the evolution of O_2 is observed only when the Pt-loaded TiO_2 is used as the photocatalyst and moisture is present in the gas phase with N_2O.[10] Recently, zeolites exchanged with various transition metal ions such as Cu^+ or Pr^{3+} have been found to act as photocatalysts for the direct decomposition of N_2O into N_2 and O_2 at ambient temperatures.[11−16] In these cases, both the electron excited to the upper empty orbital and hole simultaneously produced in the valence or inner orbital of the metal cations act as an electron and hole pair. The extremely localized electron and hole formed can thus induce unique photocatalytic reactions different from those of other semiconducting materials.

Among ion-exchanged zeolites, Ag^+/zeolites are quite unique materials since they exhibit high activities for various photochemical reactions such as the photochemical/thermal cleavage of water into H_2 and O_2,[17] photooxygen production from water,[18] photodimerization of alkanes,[19] and photocatalytic decomposition of NO_x.[20−25] Ag^+/zeolites also act as efficient thermal catalysts for deNO_x reactions such as the selective catalytic reduction (SCR) of NO_x with hydrocarbon or dimethyl ether.[26−29] However, the reactivity of Ag^+/zeolites with gaseous N_2O and especially the interaction of Ag^+ with N_2O under UV irradiation have not yet been fully investigated.

In the present work, highly dispersed Ag^+ ion catalysts were prepared within the ZSM-5 zeolite by an ion-exchange method, and comprehensive characterization of the local structure of the Ag^+ species has been carried out by in-situ XPS, XAFS (XANES and EXAFS), UV−Vis, and photoluminescence investigations. The interaction of Ag^+ with N_2O as well as the photocatalytic reactivities of Ag^+ species for the direct decomposition of N_2O have been studied by FT-IR measurements along with an analysis of the reaction products.

Experimental Section

H^+/ZSM-5 (SiO_2/Al_2O_3 = 23.8) was used as the parent zeolite. The Ag^+/ZSM-5 catalysts were prepared by a conventional ion-exchange of the corresponding H^+/ZSM-5 from an $AgNO_3$ solution with the desired Ag^+ concentration at 298 K for 24 h. After the ion-exchange, the samples were washed with distilled water and dried in air at 373 K. The silver loadings of the Ag^+/ZSM-5 catalysts were determined to be 0.5−3.9 wt % as Ag metal, using an atomic absorption spectrometer. The Ag loadings of the catalysts are shown in parentheses after the catalyst name, as in Ag^+/ZSM-5(1.4). The Ag^0/ZSM-5(2.9) catalyst was then prepared by heating the Ag^+/ZSM-5(2.9) at 673 K in the presence of a $NH_3/H_2/H_2O$ mixture at a total pressure of 30 Torr (NH_3:H_2:H_2O = 1). Cu^+/ZSM-5 (1.6) (1.6 wt % as Cu metal) was prepared by the evacuation of the Cu^{2+}/ZSM-5(1.6) at 973 K up to 10^{-5} Torr.[15] The photocatalytic decomposition reaction of N_2O was carried out with the catalysts (50 mg) in a quartz cell with a flat bottom connected to a vacuum system (10^{-5} Torr range), which was used for pretreatment and in-situ measurements of the spectra of adsorbed species. Prior to spectroscopic and photocatalytic reactivity measurements, the samples were degassed at 673 K, calcined

* Corresponding author. E-mail: anpo@ok.chem.osakafu-u.ac.jp.

10.1021/jp0302919 CCC: $27.50 © 2004 American Chemical Society
Published on Web 01/23/2004

at 673 K in the presence of 20 Torr of O_2 for 1 h, and then finally evacuated at 473 K for 1 h. Photocatalytic reactions were carried out at 298 K using a high-pressure Hg mercury lamp ($\lambda > 200$ nm) through a water filter. An UV-cut filter ($\lambda > 250$ nm) was used to examine the effect of the irradiation wavelength on the reaction. The reaction products were then analyzed by gas chromatography. The in-situ UV−Vis spectra were measured at 298 K using a double-beam digital spectrophotometer (Shimadzu UV-2200A). A $BaSO_4$ powder was used as a reference. The obtained diffuse reflectance spectra, R_d, were converted into the Kubelka−Munk function, $f(R_d)$ by using the equation $f(R_d) = (1 - R_d)^2/2R_d = k/s$, where k and s represent the absorption coefficient and scattering coefficient, respectively. $f(R_d)$ is proportional to the absorption coefficient, k, if the scattering coefficient s is assumed to be constant in the wavelength range where R_d is measured. The in-situ photoluminescence spectra of the catalyst were recorded at 298 K with a spectrofluorimeter (Spex Fluorolog II) using a quartz cell equipped with a stopcock allowing gas adsorption. The FT-IR spectra were recorded at 298 K with a FT-IR spectrometer (JASCO FT-IR 8500) using the self-supported wafers of the catalyst and CaF_2 windows, with a spectral resolution of 2 cm^{-1} and by averaging 100 scans in transmission mode. The X-ray photoelectron spectra (XPS) (Shimadzu ESCA-3200) were recorded at 298 K. A Mg Kα radiation X-ray source was used with the power at 240 W. The binding energy was calibrated with the C 1s peak at 285.2 eV. The XAFS spectra (XANES and EXAFS) were obtained at the BL-10B facility of the High Energy Accelerator Research Organization in Tsukuba. A Si(311) channel-cut crystal was used to monochromatize the X-rays from the 2.5 GeV electron storage ring. The Ag K-edge absorption spectra were recorded in the transmission mode at 298 K. The photon energy was calibrated by the edge position in the absorption spectrum of a Ag foil (25521 eV). The normalized spectra were obtained by procedures described in previous papers[30] and the Fourier transformation was performed on k^3-weighted EXAFS oscillations in the range of 3−10 $Å^{-1}$. The curve-fitting of the EXAFS data were carried out by employing the iterative nonlinear least-squares method of Levernberg[30] and the empirical backscattering parameter sets were extracted from the shell features of the silver compounds.

Results and Discussion

In-Situ Characterization of the Ag^+/ZSM-5 Catalysts. X-ray photoelectron spectroscopy (XPS) was employed as an analytical tool in order to determine the chemical state of the silver species existing within the Ag^+/ZSM-5 catalysts with 1.4 and 3.9 wt % Ag loadings. Figure 1 shows the XPS of the Ag $3d_{3/2}$ and $3d_{5/2}$ band of the Ag^+/ZSM-5 catalysts, $AgNO_3$, and the Ag metal. The Ag $3d_{5/2}$ band of the Ag^+/ZSM-5(1.4) and Ag^+/ZSM-5(3.9) catalysts appears at 370.7 and 370.5 eV, respectively. These values are quite similar to that of silver nitrate (370.1 eV) and shift to higher energy regions with respect to the Ag metal (367.9 eV), indicating that Ag^+ is the main silver component in ZSM-5. Furthermore, the Ag $3d_{5/2}$ binding energies of both the Ag^+/ZSM-5 catalysts were higher than the corresponding energy of silver nitrate. This suggests that relaxation energy of the Ag^+ ion within ZSM-5 is smaller than that of the Ag^+ ion in crystals of $AgNO_3$, i.e., the silver ions were anchored in a highly dispersed state within ZSM-5.

Figure 2 shows the Ag K-edge XANES and Fourier-transformed EXAFS spectra (FT-EXAFS) of Ag^+/ZSM-5 catalysts with different Ag loadings, the bulk Ag_2O, and Ag foil. The XANES spectra of the Ag foil and bulk Ag_2O exhibit

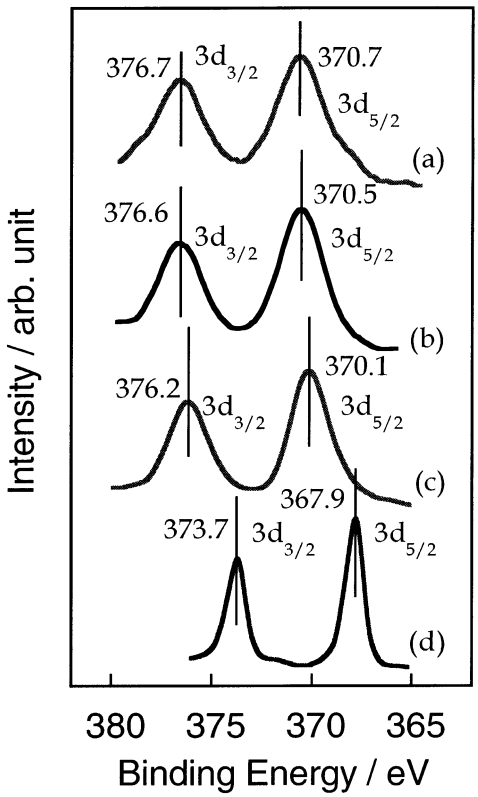

Figure 1. X-ray photoelectron spectra of Ag^+/ZSM-5 catalysts (a, b), $AgNO_3$ (c), and Ag metal (d). (a) 1.4, (b) 3.9 wt %.

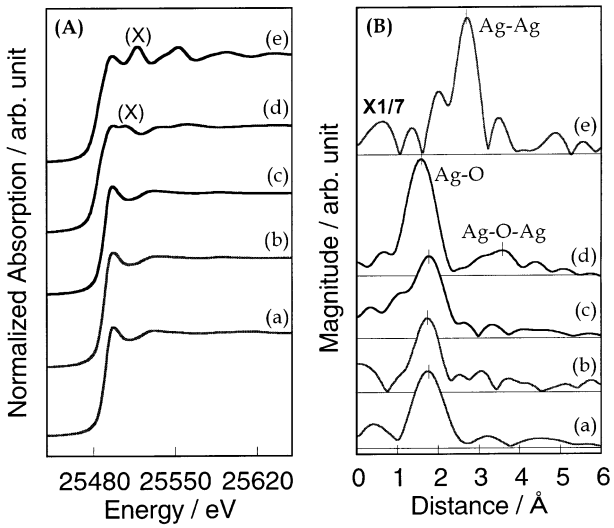

Figure 2. XANES (A) and FT-EXAFS spectra (B) of Ag^+/ZSM-5 catalysts with different Ag loadings (a∼c), Ag_2O (d), and Ag foil (e). (a) 1.4, (b) 2.9, (c) 3.9 wt %.

well-defined bands due to the multiple scattering observed at around 25530 eV (X), while the XANES spectra of the Ag^+/ZSM-5 catalysts scarcely exhibit any remarkable bands due to this effect. This implies that silver ions exist in a highly dispersed state forming neither clusters nor Ag metal or oxide crystals. As also shown in Figure 2(B), the FT-EXAFS measurements of Ag_2O exhibit two peaks at around 1.6 Å and 3.5 Å (phase shift is not corrected) attributed to the Ag−O and Ag−O−Ag bonding, respectively, while FT-EXAFS of the Ag foil exhibits an intense peak at around 2.7 Å due to the Ag−Ag bonding. However, FT-EXAFS of the Ag^+/ZSM-5 catalysts exhibits only a well-defined peak due to the neighboring oxygen

TABLE 1: The Results of the Curve-Fitting of Ag K-edge EXAFS Data for Ag^+/ZSM-5 Catalysts

sample	Ag loadings (wt %)	shell	R^a (Å)	CN[b]	$\sigma^{2\,c}$ (Å^2)
Ag^+/ZSM-5	1.4	Ag−O	2.17	1.85	0.009
	2.9	Ag−O	2.16	1.85	0.009
	3.9	Ag−O	2.16	1.88	0.010
Ag_2O		Ag−O	2.00	2.0	
Ag foil		Ag−Ag	2.88	12	

[a] R: Bond distances. [b] CN: coordination number. [c] σ^2: Debye−Waller factor.

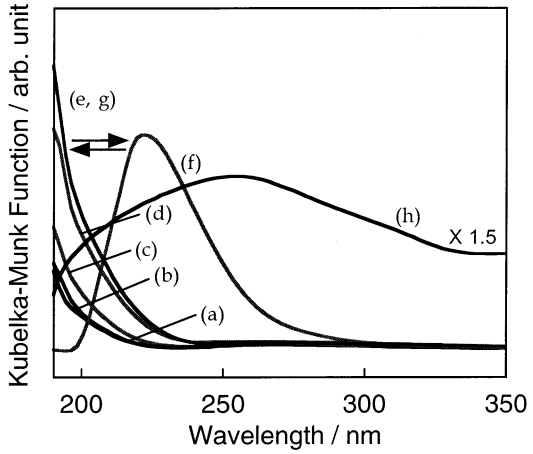

Figure 3. UV−Vis spectra of Ag^+/ZSM-5 catalysts with different Ag loadings (a−e), and Ag^0/ZSM-5 (2.9) (h), and the effect of the addition of N_2O on the UV−Vis spectrum of the Ag^+/ZSM-5 (2.9) (f, g). (a) 0.5, (b) 0.9, (c) 1.4, (d) 2.9, (e) 3.9 wt %, (f) after the addition of N_2O until the equilibrium pressure of N_2O on the catalyst reaches 1 Torr, (g) degassed for 1 h after the addition of 1 Torr of N_2O, (h) Ag^0/ZSM-5 (2.9) prepared by heating the Ag^+/ZSM-5(2.9) at 673 K in the presence of a $NH_3/H_2/H_2O$ mixture.

atoms (Ag−O) at around 1.8 Å, the intensity of the peak due to Ag−Ag or Ag−O−Ag being quite weak as compared to that of the Ag foil or Ag_2O powder. These results show that the isolated Ag^+ ions are the main silver component within the micropores of ZSM-5 and show a good agreement with the results of XANES investigations. Table 1 shows the results obtained by the curve-fitting analyses of the EXAFS spectra. The Ag−O peak exhibits an Ag−O bond length at around 2.16 Å and coordination number at around 1.9, indicating that isolated 2-coordinate silver ions are present in the pore structure of the ZSM-5 zeolite.

Figure 3 shows the UV−Vis spectra of the Ag^+/ZSM-5 catalysts with various silver loadings and the Ag^0/ZSM-5 sample prepared by the reduction of Ag^+/ZSM-5(2.9) in the presence of a $NH_3/H_2/H_2O$ mixture at 673 K. The Ag^+/ZSM-5 catalysts exhibited an intense UV absorption band at around 190 nm (the peak position of the band may exist in wavelength regions shorter than 190 nm) which is attributed to the [Kr] $4d^{10} \rightarrow$ [Kr] $4d^9 5s^1$ intraionic electronic transition on the isolated Ag^+ ion.[31] Furthermore, the intensity of the band was found to increase with an increase in the Ag loading.

Calzaferri et al.[32] have reported that three-coordinate Ag^+ at the 6-ring position and four-coordinate Ag^+ at the 4-ring position of zeolite A exhibit an absorption band due to LMCT (ligand-to-metal charge transfer) transition from oxygen lone pairs to Ag^+ at around 250 and 500 nm, respectively, by molecular orbital calculations. The electronic transition of two-coordinate Ag^+ within ZSM-5 (∼190 nm) can have a LMCT nature. However, since the absorption energy is higher than that of Ag^+ in zeolite A and more comparable to the energy of a $4d^{10} \rightarrow 4d^9 5s^1$ transition of gaseous Ag^+ ($^1D_2$ = 217 nm),[33] we have tentatively assigned the absorption at 190 nm to the d−s transition. The detailed origin of the electronic transition of the two-coordinate Ag^+ is now under investigation by molecular orbital calculations.

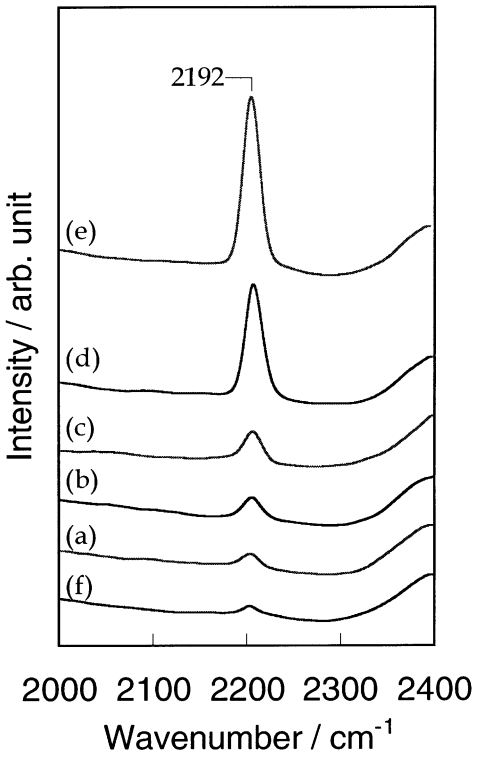

Figure 4. FT-IR spectra of CO adsorbed on Ag^+/ZSM-5 catalysts with various Ag^+ loadings (a−e) and Ag^0/ZSM-5 (2.9)(f) at 298 K. (a) 0.5, (b) 0.9, (c) 1.4, (d) 2.9, (e) 3.9 wt %, (f) Ag^0/ZSM-5 (2.9). Equilibrium pressure of CO on the catalysts: 1 Torr.

The Ag^+/ZSM-5 catalysts do not exhibit any absorption bands in wavelength regions longer than 250 nm where the absorption bands of the Ag^0 atoms, Ag_n^0 and Ag_m^{n+} clusters appear, showing that the isolated Ag^+ ions are the main silver component within the ZSM-5 zeolite. As shown in Figure 3(h), Ag^0/ZSM-5 exhibits no intense absorption band due to the Ag^+ ions at around 190 nm, while the broad absorption band due to the Ag_n^0 and Ag_m^{n+} clusters appear above 250 nm, indicating that the reduction and aggregation of the Ag^+ ions have occurred.[34]

CO adsorption measurements, which are the most widely used for IR spectroscopic characterizations of the surface Ag^+ site, were carried out at 298 K after pretreatment. As shown in the Figure 4, the addition of CO onto Ag^+/ZSM-5 led to the appearance of a typical FT-IR peak at 2192 cm^{-1} which is attributed to the formation of one-on-one Ag^+−CO adducts, and the relative intensities of the band increase with an increase in the Ag loading.[35−38] Adsorption of CO onto various Ag loadings on ZSM-5 show a positive shift of their frequencies with respect to the free CO molecules(ν_{CO} = 2143 cm^{-1}), which can be attributed to the interaction of CO (through the carbon end) with the positive electric field set by cations, i.e., the σ-donation behavior from the CO 5σ orbital to the Ag^+ ion.[39−41] No bands around 2060 cm^{-1} due to the Ag^0−CO species were observed, which implied the absence of metal silver particles on the sample. The band at 2192 cm^{-1} decreases in its intensity with a decrease in the equilibrium CO pressure, and even after evacuation of CO for 1 h, 20% of its intensity is retained.

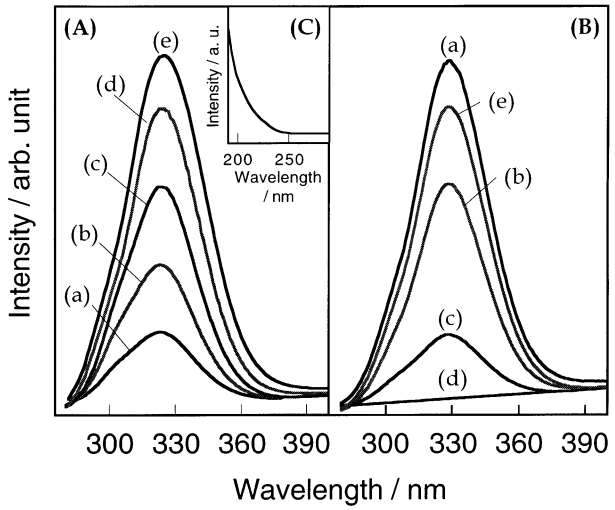

Figure 5. Photoluminescence of Ag^+/ZSM-5 with various Ag loadings (A, a−e) and effect of the addition of N_2O on the photoluminescence spectrum of Ag^+/ZSM-5 (2.9) (B) measured at 298 K. (A): (a) 0.5, (b) 0.9, (c) 1.4, (d) 2.9, (e) 3.9 wt %. (B): Equilibrium pressure of N_2O on the catalysts (a) 0.0, (b) 0.5, (c) 1.0, (d) 5.0 Torr, (e) degassed for 1 h after (d). (C): Excitation spectrum of Ag^+/ZSM-5 (2.9) monitored at 330 nm.

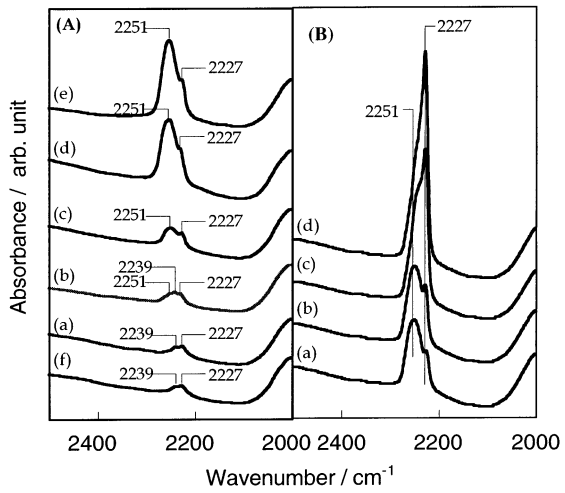

Figure 6. FT-IR spectra of N_2O adsorbed on Ag^+/ZSM-5 catalysts with various Ag loadings (A, a−e), H^+/ZSM-5 (f), and effect of the addition of N_2O on the FT-IR spectrum of Ag^+/ZSM-5 (2.9) measured at 298 K (B, a−d). (A): (a) 0.5, (b) 0.9, (c) 1.4, (d) 2.9, (e) 3.9 wt %, (f) H^+/ZSM-5; equilibrium pressure of N_2O on the catalysts: 1.0 Torr. (B): Equilibrium pressure of N_2O on the catalysts: (a) 0.5, (b) 1.0, (c) 5.0, (d) 10.0 Torr.

Evacuation at 373 K led to a strong decrease in the band intensity, disappearing completely after degassing at 423 K. Such behavior in the observed IR band is in good agreement with that of Ag^+−CO species reported in previous literature, indicating that the isolated Ag^+ ion is the main silver moiety within the Ag^+/ZSM-5.[42−45]

The Interaction of N_2O with the Ag^+/ZSM-5 Catalysts. The interaction of N_2O with the Ag^+ ions anchored within ZSM-5 was investigated by means of in-situ UV−Vis and photoluminescence measurements. As shown in Figure 3, the addition of 1 Torr of N_2O onto Ag^+/ZSM-5 led to a shift in the UV absorption band of the isolated Ag^+ ion at around 190 nm toward longer wavelength regions of around 220 nm, while the evacuation of the system at 298 K led to the complete restoration of the original absorption band. This indicates that N_2O adsorbs on the isolated Ag^+ ion, leading to a modification of the coordination sphere of Ag^+ as well as changes in the energy gap of the intraionic electronic transition ($4d^95s1 \rightarrow 4d^{10}$) of Ag^+, although the adsorption of N_2O on Ag^+ is weak and reversible.[31]

As shown in Figure 5(A), the Ag^+/ZSM-5 catalysts exhibit a photoluminescence at around 330 nm upon excitation at around 200 nm. The photoluminescence band at around 330 nm observed for these catalysts can be assigned to the radiative deactivation process of the isolated Ag^+ ion $4d^95s^1 \rightarrow 4d^{10}$ from its photoexcited state. The intensity of the photoluminescence increases proportionally with an increase in the amount of Ag loadings, without any shift in its position, suggesting that the Ag^+ ions exist in an isolated state within the Ag loading region of 0.5−3.9 wt %. As also shown in Figure 5(C), the excitation spectrum of Ag^+/ZSM-5 exhibits an absorption band at around 190 nm, where the UV absorption band of the Ag^+ ion ($4d^{10} \rightarrow 4d^95s^1$) exists, confirming that the observed photoluminescence is attributed to the presence of the isolated Ag^+. As can also be seen in Figure 5(B), the addition of N_2O onto Ag^+/ZSM-5(2.9) led to an efficient quenching of the photoluminescence, while the degassing of N_2O after the complete quenching of the photoluminescence led to the recovery of the photoluminescence to its original intensity level. These results clearly suggest that almost all of the isolated Ag^+ can interact reversibly with the N_2O molecules.

The interaction of N_2O with the Ag^+ ion was also investigated by means of an FT-IR spectrometer. As shown in the Figure 6(A), the Ag^+/ZSM-5 catalysts exhibit a specific FT-IR peak at 2251 cm^{-1} in the presence of 1 Torr of N_2O, assigned to the asymmetric stretching mode of the adsorbed N_2O.[46] The position of the peak (2251 cm^{-1}) is quite different from that of the N_2O species adsorbed onto H^+/ZSM-5 (2239 and 2227 cm^{-1}) or Ag^0/ZSM-5 (2220 cm^{-1}).[47] The intensity of the peak at 2251 cm^{-1} increases with an increase in the Ag loading while the evacuation of N_2O at 298 K led to the complete disappearance of the band, indicating that N_2O adsorbs onto the Ag^+ ion reversibly. On the other hand, as shown in Figure 6(B), the FT-IR peak at 2251 cm^{-1} does not increase in the presence of N_2O at higher than 1 Torr. However, the intensity of the peak at 2227 cm^{-1} which can be assigned to the N_2O adsorbed onto the acidic site (H^+ or silanol group) of the ZSM-5 zeolite increases in the presence of N_2O at higher than 1 Torr. In fact, the relative intensities of the peaks at 2227 cm^{-1} and 2251 cm^{-1} in the presence of N_2O at (a) 0.5, (b) 1.0, (c) 5.0, and (d) 10.0 Torr can be determined to be (a) 102, (b) 161, (c) 451, and (d) 671 a.u. for the peak at 2227 cm^{-1} and (a) 237, (b) 270, (c) 285, and (d) 274 a.u. for the peak at 2251 cm^{-1}, respectively. These phenomena can be explained by the preferential adsorption of N_2O onto the Ag^+ ion rather than H^+, i.e., after the occupation of the Ag^+ site, N_2O starts to adsorb onto the H^+ site. The addition of 1 Torr of N_2O was seen to be sufficient for the quenching of the photoluminescence of Ag^+ as well as for the complete shift of the UV−Vis band due to Ag^+ toward longer wavelength region, supporting the above results.

Photocatalytic Decomposition of N_2O on the Ag^+/ZSM-5 Catalysts. Figure 7 shows the reaction profiles of the photocatalytic decomposition of N_2O on Ag^+/ZSM-5 catalysts with different silver loadings and Ag^0/ZSM-5 at 298 K. UV irradiation of Ag^+/ZSM-5 in the presence of 1 Torr of N_2O at 298 K leads to the efficient formation of N_2 and O_2 ($N_2/O_2 = 3$). The yields of N_2 and O_2 increase with a good linearity against the UV irradiation time and also with the amount of silver loadings, while under dark condition, such formations could not be

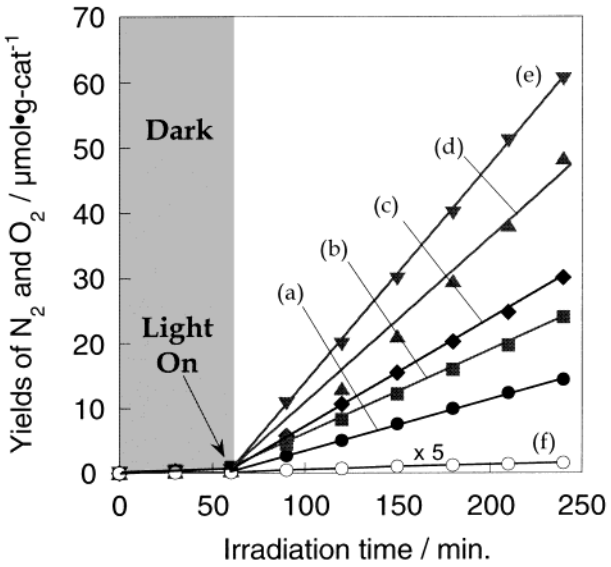

Figure 7. Reaction time profiles of the photocatalytic decomposition of N_2O into N_2 and O_2 at 298 K on Ag^+/ZSM-5 catalyst with various loadings (a−e) and Ag^0/ZSM-5 (2.9). (a) 0.5, (b) 0.9, (c) 1.4, (d) 2.9, (e) 3.9 wt %, (f) Ag^0/ZSM-5 (2.9). Equilibrium pressure of N_2O on the catalysts: 1.0 Torr.

detected. The value of the yield of photoformed N_2 molecules per total number of Ag^+ ions included in the catalyst exceeded 2.0 after prolonged UV irradiation and after this time, the decomposition of N_2O proceeded linearly with the UV irradiation time, indicating that the reaction proceeds photocatalytically. On the other hand, only a small amount of N_2 was formed on Ag^0/ZSM-5, indicating that Ag^+ ions play a significant role in the photocatalytic decomposition of N_2O. Under UV irradiation of the catalyst through an UV-cut filter (λ > 250 nm), the photocatalytic decomposition of N_2O proceeded at around 4% the rate under the full arc of the high-pressure mercury lamp. This indicates that the UV-light effective for the reaction lies in wavelength regions of 200−250 nm where the UV absorption band due to the Ag^+ ion adsorbed by the N_2O molecules exists (200−250 nm). These results show that the photoexcitation of the Ag^+ ion ($4d^{10} \rightarrow 4d^9 5s^1$) plays a significant role in the photocatalytic decomposition of N_2O on Ag^+/ZSM-5.

Figure 8 shows the effect of the loadings of Ag^+ ions on the intensity of the photoluminescence due to Ag^+, on the FT-IR spectra of the adsorbed N_2O and CO as well as the yields of the photocatalytic decomposition of N_2O on the Ag^+/ZSM-5. The relative intensities of the photoluminescence due to Ag^+ and the FT-IR peaks of N_2O and CO adsorbed on the isolated Ag^+ ions as well as the photocatalytic reactivity of the catalyst increase with an increase in the amount of silver loadings, all showing a good parallel relationship. These results indicate that the Ag^+ ion is anchored within ZSM-5 zeolite in an isolated state with an Ag loading of less than 3.9 wt %, while the photocatalytic decomposition of N_2O proceeds through the photoexcitation of the Ag^+ ion adsorbed by gaseous N_2O.

As shown in Figure 9, Ag^+/ZSM-5(2.9) shows higher photocatalytic reactivity as compared with Cu^+/ZSM-5(1.6) where the majority of Cu moieties is a linear 2-coordinate Cu^+,[15] and the N_2/O_2 ratios of the reaction products are lower for Ag^+/ZSM-5. The decrease in the reaction rate under UV irradiation was observed only for the Cu^+/ZSM-5(1.6) catalysts. These results can be attributed to the fact that the Ag^+ ions more easily desorb oxygen atoms formed during the photocatalytic reaction and in equilibrium with O_2 in the gas phase, as compared to

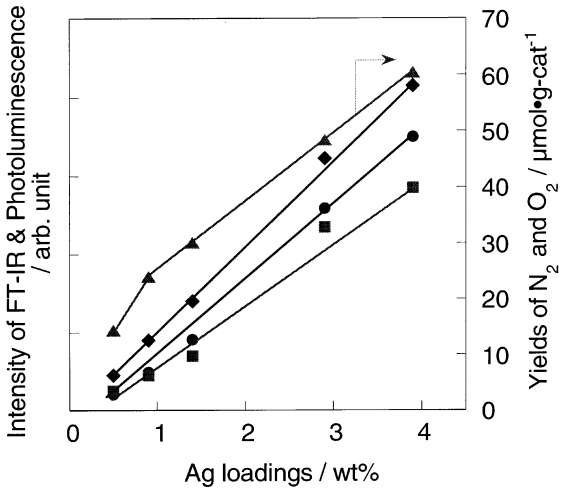

Figure 8. Effect of the Ag loadings of Ag^+/ZSM-5 catalysts on the relative intensities of FT-IR spectra of N_2O (■) and CO (●) adsorbed on the Ag^+ ion, on the intensities of photoluminescence (◆) and the reaction rate of photocatalytic decomposition of N_2O on the Ag^+/ZSM-5 (▲). FT-IR measurements and photocatalytic reactions were carried out under 1 Torr (equilibrium pressure) of corresponding added gases.

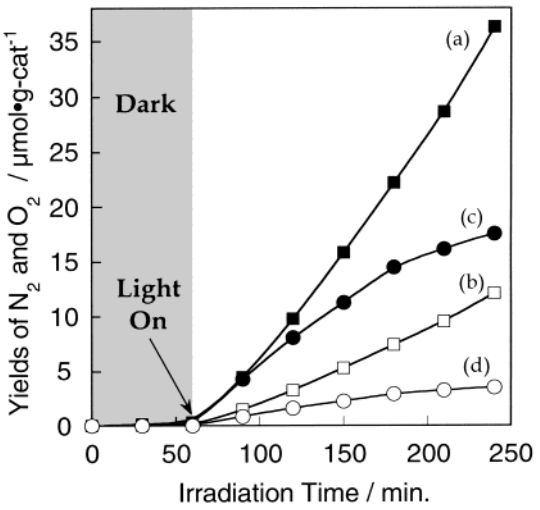

Figure 9. Reaction time profiles of the photocatalytic decomposition of N_2O into N_2 and O_2 on Ag^+/ZSM-5 (2.9) and Cu^+/ZSM-5 (1.6) catalysts at 298 K. (a) N_2, (b) O_2 on Ag^+/ZSM-5 (2.9), (c) N_2, (d) O_2 on Cu^+/ZSM-5 (1.6). Equilibrium pressure of N_2O on the catalysts: 1.0 Torr.

the Cu^+ ions.[12] ESR measurements indicated that the addition of O_2 at high pressures (> 1 Torr) did not lead to the oxidation of the Ag^+ ion to Ag^{2+} on the Ag^+/ZSM-5 catalyst, in clear contrast to the easy oxidation of Cu^+ to Cu^{2+} on the Cu^+/ZSM-5 catalyst.[48] It was, thus, elucidated that the Ag^+ ions are chemically stable even under an oxidative atmosphere as well as under photocatalytic reactions. This can be considered a major advantage in using the Ag^+/ZSM-5 catalyst as a potential photocatalyst for the direct decomposition of N_2O at normal temperatures. Another advantage is the lower pretreatment temperature of the original Ag^+/ZSM-5 sample at just 473 K as compared to the preparation of the copper ion catalyst which requires evacuation of the Cu^{2+}/ZSM-5 sample at temperatures higher than 973 K in order to produce Cu^+ ions as active species.[15,49]

From these findings, it was concluded that the two-coordinate isolated Ag^+ ions are selectively produced within the ZSM-5 zeolite by an ion-exchange method, and N_2O reversibly adsorbs on the isolated Ag^+ ion. In-situ UV−Vis, FT-IR, and photo-

luminescence investigations elucidated the significant role the photoexcitation of the absorption band of the isolated Ag^+ ion in the presence of N_2O plays in the reaction characterized by the intraionic electronic transition of Ag^+ ion ($4d^{10} \rightarrow 4d^9 5s^1$). It is considered that an electron transfer of the 5s electron of the photoexcited Ag^+ into the antibonding molecular orbital (LUMO) of N_2O initiates the decomposition of N_2O to produce N_2 and O_2. Similar reaction mechanisms are proposed for the photocatalytic decomposition of NO on Ag^+/ZSM-5[24,25] as well as for the photocatalytic decomposition of N_2O on Cu^+/ZSM-5,[11,12] where an "s" electron transfer of the photoexcited metal ions into the reactant molecules plays an important role.

Conclusions

In-situ UV−Vis, photoluminescence, FT-IR, XPS, and XAFS investigations of the Ag^+/ZSM-5 catalysts prepared by an ion-exchanged method indicated that two-coordinate isolated Ag^+ ions exist within the ZSM-5 zeolite cavities, exhibiting a typical photoluminescence spectrum at around 330 nm upon excitation at around 200 nm. The added N_2O molecules reversibly adsorbed on the isolated Ag^+ species, exhibiting a characteristic UV−Vis absorption band at 220 nm, as well as an IR absorption peak at 2251 cm^{-1}.

The photocatalytic decomposition of N_2O proceeds efficiently on the Ag^+/ZSM-5 catalysts leading to the formation of N_2 and O_2 even at an ambient temperature. Investigations of the in-situ UV−Vis and photoluminescence spectra of the Ag^+/ZSM-5 catalyst as well as the effective wavelengths of irradiated UV light on the reaction showed that the photoexcitation of the two-coordinated isolated Ag^+ ion ($4d^{10} \rightarrow 4d^9 5s^1$) plays a significant role in the reaction.

Acknowledgment. M. Anpo is much indebted to Tosoh Corporation for kindly providing the ZSM-5 samples.

References and Notes

(1) Anpo, M. In *Proc. 12th International Congress on Catalysis*, Spain, Granada, 2000; p 157.
(2) Anpo, M. In *Green Chemistry*; Tundo, P., Anastas, P., Eds.; Oxford University Press: New York, 2000; p 1.
(3) Joseph, H. H.; Matthew, A. S.; Robert, J. D. *J. Catal.* **2000**, *190*, 247.
(4) Uetsuka, H.; Mizutani, N.; Hayashi, H.; Onishi, H.; Kunimori, K. *Catal. Lett.* **2000**, *59*, 165.
(5) Luo, J. Z.; Gao, L. Z.; Leung, Y. L.; Au, C. T. *Catal. Lett.* **2000**, *66*, 91.
(6) Yamada, K.; Pophal, C.; Segawa, K. *Microporous Mesoporous Mater.* **1998**, *21*, 549.
(7) Higashimoto, S.; Nishimoto, K.; Ono, T.; Anpo, M. *Chem. Lett.* **2000**, 1160.
(8) Rusu, C. N.; Yates, J. T. *J. Phys. Chem.* **2001**, *105*, 2596.
(9) Kudo, A.; Nagayoshi, H. *Catal. Lett.* **1998**, *52*, 109.
(10) Kudo, A.; Sakata, T. *Chem. Lett.* **1992**, 2381.
(11) Ebitani K.; Morokuma, M.; Kim, J.-H.; Morikawa, A. *J. Catal.* **1993**, *141*, 725.
(12) Ebitani K.; Morokuma, M.; Kim, J.-H.; Morikawa, A. *J. Chem. Soc., Faraday Trans.* **1994**, *90*, 377.
(13) Ebitani, K.; Hirano, Y.; Morikawa, A. *J. Catal.* **1995**, *157*, 262.
(14) Anpo, M.; Matsuoka, M.; Hanou, K.; Mishima, H.; Yamashita, H.; Patterson, H. H. *Coord. Chem. Rev.* **1998**, *171*, 175.
(15) Yamashita, H.; Matsuoka, M.; Tsuji, K.; Shioya, Y.; Anpo, M.; Che, M. *J. Phys. Chem.* **1996**, *100*, 397.
(16) Anpo, M.; Matsuoka, M.; Mishima, H.; Yamashita, H. *Res. Chem. Intermed.* **1997**, *23*, 197.
(17) Jacobs, P. A.; Uytterhoeven, J. B.; Beyer, H. K. *J. Chem. Soc., Chem. Commun.* **1977**, 128.
(18) Calzaferri, G.; Hug, S.; Hugentobler, T.; Sulzberger, B. *J. Photochem.* **1984**, *26*, 109.
(19) Ozin, G. A.; Hugues, F. *J. Phys. Chem.* **1982**, *86*, 5174.
(20) Anpo, M.; Zhang, S. G.; Mishima, H.; Matsuoka, M.; Yamashita, H. *Lett. Nuovo Cimento* **1997**, *39*, 1641.
(21) Anpo, M. *Catal. Today* **1997**, *19*, 159.
(22) Anpo, M.; Zhang, S. G.; Mishima, H.; Matsuoka, M.; Yamashita, H. *Catal. Today* **1997**, *39*, 159.
(23) Kanan, S. M.; Omary, M. A.; Patterson, H. H.; Matsuoka, M.; Anpo, M. *J. Phys. Chem.* **2000**, *104*, 3507.
(24) Matsuoka, M.; Matsuda, E.; Tsuji, K.; Yamashita, H.; Anpo, M. *Chem. Lett.* **1997**, 375.
(25) Matsuoka, M.; Matsuda, E.; Tsuji, K.; Yamashita, H.; Anpo, M. *J. Mol. Catal. A* **1996**, *107*, 399.
(26) Sato, S.; Yu-u, Y.; Yahiro, H.; Mizuno, N.; Iwamoto, M. *Appl. Catal.* **1991**, *70*, L1.
(27) Miyadera, T.; Abe. A.; Muramatsu, G.; Yoshida, K. In *Proc. Symp. Environ. Conscious Mater.*, Japan, Tokyo, 1993; p 405.
(28) Miyadera, T. *Appl. Catal. B* **1993**, *2*, 199.
(29) Aoyama, N.; Yamashita, Y.; Abe, A.; Takezawa, N.; Yoshida, K. *Phys. Chem. Chem. Phys.* **1999**, *1*, 3365.
(30) Tanaka, T.; Yamashita, H.; Tsuchitani, R.; Funabiki, T.; Yoshida, S. *J. Chem. Soc., Faraday Trans. 1* **1998**, *84*, 2987.
(31) Texter, J.; Gonsiorowski, T.; Kellerman, R. *Phys. Rev. B* **1981**, *23*, 4407. (b) Texter, J.; Kellerman, R.; Gonsiorowski, T. *J. Phys. Chem. B* **1986**, *90*, 2118.
(32) Esifer, R.; Rytz, R.; Calzaferri, G. *J. Phys. Chem. A* **2000**, *104*, 7473.
(33) Donald, S. Mc. In *Electronic spectra of molecules and ions in crystals*; Academic Press: New York, 1959; p 175.
(34) Ozin, G. A.; Hugues, F.; Matter, S. M.; McIntosh, D. F. *J. Phys. Chem.* **1983**, *87*, 3445.
(35) Hadjiivanov, K. *Microporous Mesoporous Mater.* **1988**, *24*, 41.
(36) Davydov, A. In *IR Spectroscopy Applied to Surface Chemistry of Oxides*; Nauka: Novosibrisk, 1984.
(37) Hadjiivanov, K.; Vassileva, E.; Kantcheva, M.; Klissurski, D. *Mater. Chem. Phys.* **1991**, *28*, 357.
(38) Huang, Y. Y. *J. Catal.* **1974**, *32*. 482.
(39) Bordiga, S.; Palomino, G. T.; Arduino, D.; Lamberti, C.; Zecchina, A.; Areán, C. O. *J. Mol. Catal.* **1999**, *146*, 97.
(40) Fajans, K. *Naturwissenschaften* **1923**, *11*, 165.
(41) Hurlburt, P. K.; Pack, J. J.; Luck, J. S.; Dec, S. F.; Webb, J. D.; Anderson, O. P.; Strauss, S. H. *J. Am. Chem. Soc.* **1994**, *116*, 10003.
(42) Pestryakov, A. N.; Davydov, A. A.; Kurina, A. *Russ. J. Phys. Chem.* **1988**, *62*, 1813.
(43) Baumann, J.; Beer, R.; Calzaferri, B.; Waldeck, B. *J. Phys. Chem.* **1989**, *93*, 2292.
(44) Baba, T.; Akinaka, N.; Nomura, M.; Ono, Y. *J. Chem. Soc., Chem. Commun.* **1992**, 339.
(45) Jacobs, P. A.; Uytterhoeven, J. B.; Beyer, H. K. *J. Chem. Soc., Faraday Trans. 1* **1977**, *73*, 1755.
(46) Zhang, W.; Jia, M.; Yu, J.; Wu, T.; Yahiro, H.; Iwamoto, *M. Chem. Mater.* **1999**, *11*, 920.
(47) Matsuoka, M.; Ju, W. S.; Anpo, M. *Chem. Lett.* **2000**, *6*, 626.
(48) Giamello, E.; Murphy, D.; Magnacca, G.; Morterra, C.; Shioya, Y.; Nomura, T.; Anpo, M. *J. Catal.* **1992**, *136*, 510.
(49) Anpo, M.; Matsuoka, M.; Shioya, Y.; Yamashita, H.; Giamello, E.; Morterra, C.; Che, M.; Patterson, H. H.; Webber, S.; Ouellette, S.; Fox, M. A. *J. Phys. Chem.* **1994**, *98*, 5744.